Article

A Multi-channel Structured 3D Chip for Highly Sensitive Pathogenic Bacteria Detection Based on Fast DNA-programmed Signal Polymerization

Junman Chen, Zhijun Huang, Zewei Luo, Qiaoling Yu, Ya Xu, Xiaqing Wang, Yongxin Li, and Yixiang Duan

Anal. Chem., **Just Accepted Manuscript** • DOI: 10.1021/acs.analchem.8b02650 • Publication Date (Web): 18 Sep 2018

A Multi-channel Structured 3D Chip for Highly Sensitive Pathogenic Bacteria Detection Based on Fast DNA-programmed Signal Polymerization

Junman Chen,[†] Zhijun Huang,[†] Zewei Luo,[†] Qiaoling Yu,[†] Ya Xu,[†] Xiaqing Wang,[†] Yongxin, Li,[‡] Yixiang Duan*[†]

[†]*Research Center of Analytical Instrumentation, Key Laboratory of Bio-resource and Eco-environment, Ministry of Education, College of Life Sciences,* [‡]*West China School of Public Health, Sichuan University, Chengdu P. R. China, 610065*

*Corresponding author: Yixiang Duan
E-mail: yduan@scu.edu.cn
Tel: +86 28-8541-8180

Abstract

The threat of food safety and the limited analytical methods with high-performance promote the growing interest in the development of pathogenic bacteria biosensors. This study presents a pathogenic bacteria biosensing system, where a novel three-dimensional (3D) chip acts as analytical carrier and DNA-programmed hybridization chain reaction (HCR) causes signal amplification. The 3D chip is designed featuring a compact multi-channel structure. It has large surface area for sensitive sensing, and exhibits multiple functions of target capture, separation, rinse and signal detection to simplify the analysis processes. HCR, which enables fluorophores polymerization, is designed as two signal amplification modes, each with unique advantages. Mode I achieves highly sensitive detection in a "sandwich" assay format, in which a long HCR amplified probe is used to boost the fluorescence signal. In Mode II, the assembly of HCR is performed on the inner surface of 3D chip. Especially, a group of rapid assembly HCR sequences is proposed, of which the assembly time as short as 15 minutes stands out among the related works previously reported. Under the optimal conditions, the proposed biosensing system has the limits of detection (LOD) of 4 cfu/mL and 8 cfu/mL in Mode I for *Staphylococcus aureus* detection and in Mode II for *Salmonella enterica* Typhimurium detection, respectively. The specificity and the real sample applications are evaluated. This multi-channel structured 3D chip based on HCR signal amplification has potential applications in food safety monitoring and biosensor development.

Of all contaminants in food and water, pathogenic bacteria pose a serious threat to public health and financial stability. In China alone, the Chinese National Health Commission statistically reported 5,926 cases of foodborne illness with 3,181 cases caused by pathogenic bacteria in 2015.[1] The current culture-based methods have been used as gold standard.[2] However, the time-consuming multi-step operations involved in those methods remain as the major hindrances for food safety assessment process. As an alternative, nucleic acid-based molecular detection methods, such as polymerase chain reaction (PCR), real-time PCR, multiplex PCR, have been widely used for foodborne pathogen detection in resource-rich settings.[3] Nevertheless, their availability in resource-limited settings is restricted due to the time-consuming specimen collection, lack of bulky and advanced infrastructure, complex nucleic acid purification and isolation.[4] Therefore, it is imperative to develop processing-simplified systems with simple devices. Especially, methods that leave out sample processing and directly target the whole bacterial cell are desirable.[5]

In recent years, the development of biosensors has been propelled by demands in the field of public health.[6] Optical biosensors attract much attention on account of their sensitive, specific, rapid and easy-to-use characteristics. Among them, some good examples of fluorescent biosensors,[7,8] surface plasma resonance (SPR) biosensors,[9] and surface-enhanced Raman scattering (SERS) biosensors,[10] have been reported. Although those biosensors are designed based on different principles, most of them contain the same working pattern and processes, including target capture, separation, rinse, signal amplification and detection. Importantly, these processes have two major challenges that impede the further development of bacterial cell biosensors. On one hand, target bacteria in complex food matrices usually need to be captured, separated, labeled, rinsed and detected in different steps, which leads to inconvenient manipulation and cumbersome assay processes.[11] On the other hand, sensitivity is crucial in biosensor construction. However, some biosensors with solid support substrate usually have low surface area, resulting in limited area for ligand anchoring, thus leading to low target capturing.[12] This leads to unsatisfactory sensitivity when detecting pathogenic bacteria sample with low target concentration. Magnetic beads are usually used to separate and concentrate the target in order to amplify signal, but it requires complex processes.[13] To overcome these limitations, three-dimensional (3D) structured analytical carriers or biosensors have appeared in recent years. A well designed 3D system provides a compact structure, a large surface area for molecule immobilization and recognition,[14] an efficient mass transfer that enables large sample size,[11,13,15] and good flexibility in light path design.[14] In this context, we propose a novel multi-channel structured 3D chip as an analytical carrier to meet the challenges mentioned above.

Along with analytical carrier, analytical strategy is also important in biosensor construction. Analytical strategies with DNA-programmed signal amplification have been widely used, some of which were constructed to detect pathogenic bacteria.[16-18] In these strategies, hybridization chain reaction (HCR), first put forward by Pierce and Dirks, is a cascade of hybridization reaction triggered by an initiator strand in enzyme-free environment at room temperature.[19,20] The kinetically trapped hairpin monomers can coexist but do not hybridize with each other on an experimental time scale, while exposure to initiator strand can trigger the system to propagate a chain reaction of hybridization event. By modifying the hairpin monomers with functional ligands such as fluorophore,[21] biotin[22] and quantum dots,[23] HCR enables a cascade of polymerization with ability of signal amplification. Some good examples have demonstrated that HCR can be utilized in biosensors with solid support substrate for signal amplification.[22,24,25] Inspired by these characteristics of HCR, and in order to assess the analysis ability of 3D chip, two different modes of

analytical strategy are carried out in the sensing system.

In this work, a multi-channel structured 3D chip for pathogenic bacteria detection based on HCR is proposed. As an analytical carrier, the 3D chip can simplify the analysis process, and has multi-channel structure to improve the sensitivity. Two analytical strategies corresponding to two modes in this system are designed for signal amplification. In Mode I, a long HCR amplified probe is used in "sandwich" assay. This long amplified probe is expected to enlarge the fluorescence signal, and hence warrant high sensitivity. In Mode II, the inner surface of 3D chip acts as substrate for HCR assembly. A group of HCR sequences with rapid assembly speed is proposed, which stands in contrast to the reported HCR sequences that usually need several hours to assemble. *S. aureus* and *S.* Typhimurium are employed as targets for Mode I and Mode II, respectively, to evaluate the analytical performance of the proposed biosensing system.

Experimental Section

Reagents and materials are presented in Supporting Information

Multi-channel 3D Chip fabrication

A polymethyl methacrylate (PMMA) sheet (thickness of 2 mm, Sumitomo, Japan) was used to fabricate 3D chips. The multi-channel 3D chip was fabricated via laser technique by the Jizhi Laser Precision Products Co. Ltd (Guangdong, China) to realize our design. Briefly, the PMMA sheet was cut into a disc shape (Φ=4 mm, thickness=2 mm) by continuous laser with a power of 65 w, voltage of 220V±10% at 25℃ and 88% moisture content. The disc was fixed by a switch type clamping system with a location error of ±0.1~ 0.2 mm, and 89 channels (Φ=0.15±0.008 mm) were cut into it by pulse laser with a power of 40 W, voltage of 220 V±10% at 25℃ and 80% moisture content. Figure S-1 shows the plane-view SEM image of the 3D chip.

Polyacrylamide gel electrophoresis

Polyacrylamide gel electrophoresis (PAGE) was used in this work to test and verify the behavior of DNA assembly. The assembly effect of HCR, as well as the principle of the two modes for signal amplification, were proved by PAGE analysis. Six microliter sample mixed with loading buffer was loaded into 10% polyacrylamide gel. The electrophoresis was driven by a constant voltage of 120 V for suitable time in 1×TAE buffer. After being stained for 15 min, the gel was imaged by a C300 system (Azure Biosystems, USA).

Chip modification

In Mode I and Mode II, the 3D chip was modified with capturing aptamer and initiator strand (Is), respectively. At first, the 3D chip was ultrasonically cleaned in 1 mM nitric acid solution and 1 mM NaOH solution, respectively, for 1 h. After thoroughly rinsing with ultrapure water at a velocity of 16 mL/min for 10 min with a peristaltic pump, the 3D chip was used immediately or stored in a desiccator. Then the 3D chip was modified with amino-modified DNA by using the PEI-GA surface chemistry protocol.[26] PEI was firstly modified on the 3D chip, offering amino binding sites. GA acted as crosslinking agent to connect PEI and amino-modified DNA. The cleaned 3D chip was coated with amine groups by incubating in 0.2% (w/w) PEI for 1 h. After pumping ultrapure water at a velocity of 0.5 mL/min for 15 min, the amine-modified 3D chip was activated by 1% (w/v) GA for 30 min, and then rinsed with ultrapure water by

peristaltic pump at 0.5 mL/min for 30 min.[26] Next, the activated 3D chip was incubated with 1 μM NH_2-modified capturing aptamer or NH_2-modified Is overnight at 4℃ to covalently immobilize the NH_2-DNA onto the inner surface of the 3D chip. However, the positively charged amino groups in PEI also absorb the negatively charged phosphate backbone of DNA through electrostatic interaction.[27] Previous studies have shown that the DNA absorbed on PEI by such non-specific interaction is unstable and could be quickly desorbed in buffer with high salt concentration.[28] Thus, the non-specifically absorbed NH_2-DNA was twice washed off by binding buffer with 600 mM NaCl for 10 min. The chip was then blocked by incubating with 0.2% BSA solution (prepared in binding buffer) for 1 h. After pump rinse with binding buffer at 0.5 mL/min for 5 min, the 3D chip was stored at 4℃ and used within one week. For Mode II, after the above steps, the 3D chip was incubated with 1.5 μM aptamer for 30 min to form the Is-aptamer double strand, and then pump rinsed with binding buffer at 0.5 mL/min for 10 min before use.

Process for detection of pathogenic bacteria in 3D chip assay

In a typical detection process, ten milliliter sample containing bacteria in binding buffer was pumped into the 3D chip at 0.33 mL/min by a micro syringe pump (Longer Pump, China), which was followed by a thorough washing by binding buffer at a velocity of 0.5 mL/min for 10 min. Then for Mode I, the 3D chip was filled with the long amplified probe and incubated at room temperature for 30 min. The long amplified probe was assembled in advance before the assay: 0.5 μM initiator strand with aptamer (Is@aptamer), 4 μM TAMRA modified hybridization probe (H1) and 4 μM TAMRA modified hybridization probe (H2) were mixed and annealed before a 12 hour's incubation at room temperature. For Mode II, the 3D chip was filled with 5 μM H1 and H2, and incubated at room temperature for 15 min. Finally, the unbound H1 and H2 were washed away with binding buffer at a pumping velocity of 0.5 mL/min for 10 min. The fluorescent signal was measured by home-made *in-situ* laser-induced fluorescence (LIF) system, which was basically same as our previous work.[14,29] Supporting Information contains the details of LIF system setup.

■ Results and Discussion

• Design idea of the 3D chip

In this work, the multi-channel structured 3D chip as analytical carrier features superiority for bacterial cell analysis. It enables mass transfer for large volume sample; offers large sensing area for target binding; possesses good flexibility in optical light path; and simplifies the analysis processes. First, the inner diameter of channels on the 3D chip is approximately 150 μm. Compared with the traditional analytical carrier in the form of a single quartz tube, the smaller inner diameter makes the 3D chip more efficient to capture target bacteria onto the inner surface of the channels. The number of target cells tending to colloid with the inner surface of two different channels was simulated by COMSOL 5.3a. As shown in Figure 1a, it rapidly raises with sampling time in the thinner channel (150 μm inner diameter), while a slow growth is observed in the thick channel (2 mm inner diameter). Under the action of viscous force and fraction, the more target cells collide with the inner surface, the more chances for them to be captured by the ligand anchoring on the inner surface. Such multi-channel structure makes the 3D chip an appropriate analytical carrier for large volume sample with low concentration. Second, for most of the biosensors with solid support substrate, the traditional tube or plane supports made of glass[29], polymer[12,30] and silicon[10,31], are usually used. Compared with those types of design, the 3D chip has larger surface area in the same excitation area (Figure 1b), offering more space for ligand anchoring. This will increase the chance to capture the targets, and thus improve the sensitivity. A comparison between 3D chip and a PMMA sheet was made to illustrate the advantage of the former. *S. aureus* was detected by using the 3D chip and PMMA

sheet as analytical carrier, respectively. A typical "sandwich" assay was performed in these analytical carriers as described in Figure S-3. The result shown in Figure 1c indicates that the structure of 3D chip, which offers more surface area for target capturing, contributes to obvious signal enhancement. Third, for an analytical carrier, our previous work has demonstrated that a 3D bundle of eight capillaries performs better than a 2D array of capillaries in *in-situ* LIF system because of the flexible light path ability in the former design.[14] In this work, we further improve the 3D bundle of eight capillaries into a multi-channel structured 3D chip, which is actually a bundle of 89 channels. This compact structure of 3D chip provides optimal condition for optical detection because it can increase the efficiency of laser excitation and fluorescence collection. Fourth, by integrating in a syringe pump or a peristaltic pump system, multi-step analytical processes can be executed conveniently in the analytical carrier. The targets are captured and separated onto the inner surface of 3D chip when the large volume sample is pumped through. The labeled probe can also be pumped into the 3D chip for probe incubation. The unbound free probe and other substances can be rinsed away by pumping through buffer. All of the processes can be finished by changing the inlets of the pump. This makes the analytical assay convenient and simple. (Figure 1d).

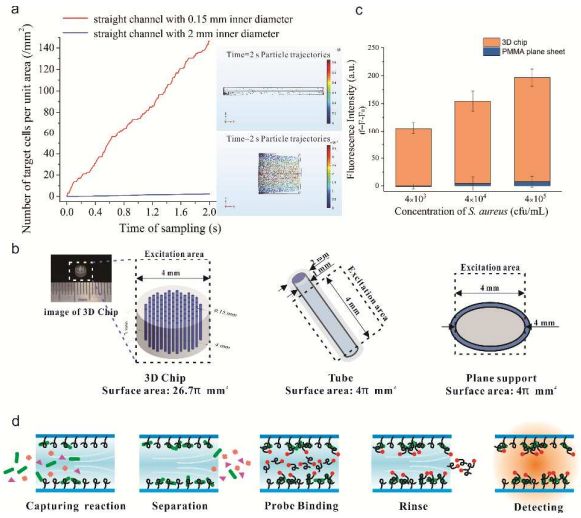

Figure 1. Characteristic features of the 3D chip used in this study. **(a)** COMSOL multiphysics (COMSOL 5.3a) simulation of the number of target cells tending to colloid with inner surface per unit area. Key boundary condition and parameters: Entry velocity = 0.33 mL/min, target cell number passing through the channel = 10000, target cell size = 5 μm. Insets are particle trajectories with the scales showing the velocity of target cells respectively. **(b)** Illustration of 3D chip (left) comparing with traditional single tube analytical carrier (middle) and plane support (right). The total area of inner surface of the 3D chip is calculated as 26.7π mm^2, while surface areas of the other two are 4π mm^2. **(c)** A comparison between 3D chip and PMMA sheet analytical carrier when detecting *S. aureus* with different concentrations. **(d)** The analytical processes occurred in the 3D chip.

- **Principle of two modes for signal amplification**

Along with the 3D chip analytical carrier, two modes of analytical strategy based on HCR signal amplification are designed in the pathogenic bacteria biosensing system, as illustrated in Figure 2. In Mode I (Figure 2a), a "sandwich" assay is processed, where targets are captured by the aptamer anchoring on the inner surface of 3D chip. Typically, a long amplified probe is prepared based on HCR. Exposure to an initiator strand opens the hairpin structure of H1, and releases the hybridization energy. Then, H1 and H2

polymerize non-covalently to form a long nicked double helices analogou.[19] Here, a single strand named as Is@aptamer with initiating function at 3' end and recognition function at 5' end is used. Since H1 and H2 are modified with fluorophore, these assembled double helices analogue can act as long amplified probes, which are expected to enlarge fluorescent signal and improve sensitivity.

Mode II (Figure 2b) is a novel signal amplification mode designed to further confirm the performance of 3D chip analysis carrier. Specifically, the HCR initiator strand (Is) is anchored on the inner surface of 3D chip, and blocked by aptamer. After incubation with target bacterial cells and subsequent rinse, the aptamer is taken away and Is is exposed. Then, H1 and H2 are added to perform HCR on the inner surface of 3D chip. It is worth noting that HCR process with rapid assembly speed is critical in this mode, otherwise it would take long time to detect bacteria in Mode II. HCR has been applied in plenty of biosensors so far, but long assembly time (usually couple of hours) is needed in most of reported works.[24,32,33] Here we present a group of HCR sequences with rapid assembly speed, which makes Mode II perform ideally.

DNA sequences used in this work are listed in Table S-1

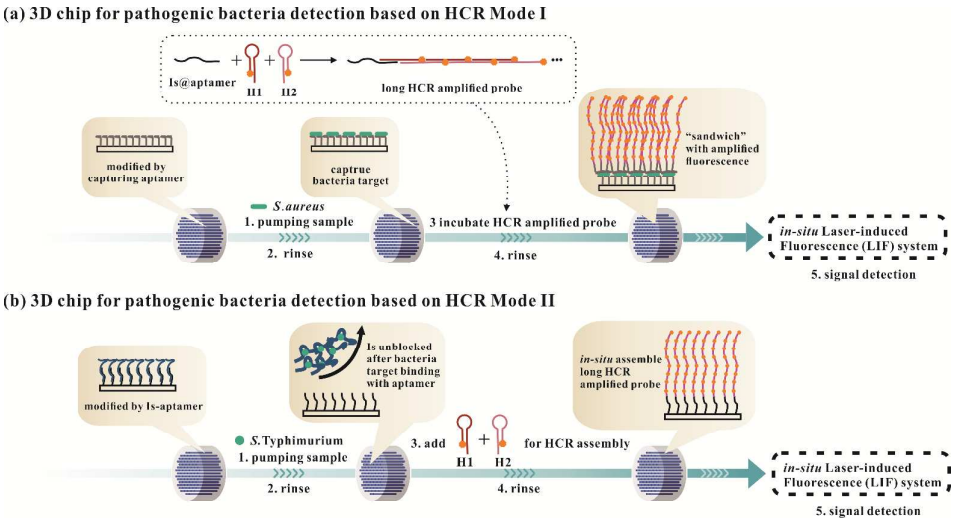

Figure 2. The principle for pathogenic bacteria analysis in this work. In both Mode I (a) and Mode II (b), after four-step processes of sample pumping, rinse, probe binding, a home-made *in-situ* laser-induced fluorescence (LIF) system was used to detect the signal (shown in Figure S-2).

- **3D chip for pathogenic bacteria detection based on HCR Mode I**

Confirmation of HCR amplified probe assembly. The HCR sequences used in Mode I were adopted from Dirks et. al (2004)[19] and the assembly was confirmed by PAGE analysis. As shown in Figure 3a, H1 and H2 coexist without Is@aptamer, while the hairpins polymerize in the presence of Is@aptamer. Specially, for the sample in lane 1, H1, H2 and Is@aptamer were mixed and annealed before assembly incubation; while for the sample in lane 2, the three sequences were mixed and directly incubated at room temperature. It is obvious that annealing process before incubation benefits the assembly effect and helps the polymerization reaction to get relatively uniform long strands.

Optimization of experimental conditions. In order to obtain optimum performance, the conditions of chip modification, long amplified probe assembly and the amount of probe used, as well as the analysis time were optimized. For the chip modification, in order to optimize the concentration of treated

amino-modified DNA and also to investigate the washing effect of non-specific absorption, the 3D chip was treated with different concentrations of amino-modified DNA from 0.1 μM to 2 μM and washed twice by binding buffer with 600 mM NaCl. The amount of amino-modified DNA was measured by ultraviolet absorption spectrum, and the data was analyzed as shown in Figure S-4. The result indicates that twice washing by high salt buffer can thoroughly desorb the non-specifically absorbed DNA. Treating the 3D chip with 1 μM amino-modified DNA guarantees its effective fixing amount to reach saturation and gives a relatively high effective fixing ratio (26.2%) comparing with 2 μM amino-modified DNA treatment (13.3%). Consequently, one micromole per liter amino-modified DNA was used to modify 3D chip, which was followed by twice washing by high salt buffer.

For the long amplified probe assembly, the incubation was carried out after the annealing process. The incubation time was optimized as shown in Figure S-5a. The HCR assembly is finished after 12 h and keeps stable for at least three days, which means that the long amplified probe can be assembled in advance. The molar ratio of Is@aptamer and H1/H2 was also optimized. Figure S-5b indicates that Is@aptamer with eightfold H1/H2 can fully complete the assembly. Then, the exact amount of long amplified probe used in the 3D chip experiment Mode I was ascertained. Here different concentrations of Is@aptamer were mixed and annealed with eightfold H1 and H2 before incubation at room temperature for 12 h. Then, the different concentrations of long amplified probe were used in Mode I 3D chip analysis to detect *S. aureus*. Figure S-6 shows that 0.5 μM Is@aptamer with 4 μM H1 and H2 can assemble long amplified probes satisfied for *S. aureus* detection.

Since aptamer was used as recognizing bioreceptor in this work, it took time for aptamer to bind with target bacterial cell. As illustrated in Figure 2a, Mode I involves five steps, where the first step "pumping sample" and the third step "incubate HCR amplified probe" take up most of the analysis time. Thus, the analysis time of these two steps were investigated. Figure 3b indicates that a 10 mL sample pumped through the 3D chip in at least 30 min (with velocity slower than 0.33 mL/min) would be appropriate. And a 30-minute incubation time for probe-target interaction is sufficient to reach the maximum fluorescence value.

Analytical performance of Mode I. With the optimized parameters above, Mode I was evaluated regarding its analytical performance for detecting *S. aureus*. In order to prove the signal amplification effect of HCR, the HCR-based "sandwich" assay and a traditional "sandwich" assay were carried out in parallel. In the traditional "sandwich" assay, the probe was assembled without H2, implicating that Is@aptamer and H1 formed a single labeled probe instead of a long amplified probe (illustrated in Figure S-3). The fluorescence spectra and corresponding calibration curves are shown in Figure 3c. The traditional "sandwich" assay presents a limit of detection (LOD) of 12 cfu/mL. (The LOD was calculated as by $3\delta_b$/slope. δ_b is the standard deviation when detecting buffer.) This good sensitivity owes to the unique structure of 3D chip used. A substantial enhancement of fluorescence signal is obtained in HCR-based "sandwich" assay comparing with the traditional one, and the corresponding LOD is 4 cfu/mL. To define a positive result, we used $3\delta_b$ (75 a.u.) as reference. Reliability was evaluated by recovery analysis in real sample matrix using the standard spiking experiment. Commercial non-fat milk powder and raw ground pork were purchased from local supermarket. The sample preparation and measurement methods are stated in Supporting Information. The spiked concentration (C1) of *S. aureus* was determined by classical counting method. Fluorescence signals measured by the proposed biosensor, and the calibration curve in Figure 3c were used to calculate the measured concentration (C2). The analysis result in Table S-2 shows no significant difference between the two methods with the recovery ranging from 87.5% to 101.1%. The

spiked *S. aureus* was detected as positive result. This indicates that the 3D chip biosensor based on HCR Mode I has potential for practical food analysis. Specificity of the biosensor depends on the affinity of the aptamer and was evaluated by detecting other ten pathogenic bacteria. As shown in Figure S-7a, the biosensor fails to tell distinct difference between different strains of *S. aureus*. Although the signal difference between target and other kinds of bacteria is distinct, these other kinds of bacteria can also lead to a certain net signal. According to the aptamer SELEX work reported by Cao et.al.,[34] the individual *S. aureus* aptamer has limited ability for strain discrimination. And a combined use of multiple *S. aureus* aptamers is potentially useful to improve the binding capacity of aptamer biosensors.[34] It is expected that the 3D chip can be used for this exploration by anchoring different *S. aureus* aptamers into different channels, and this work is ongoing in our progress.

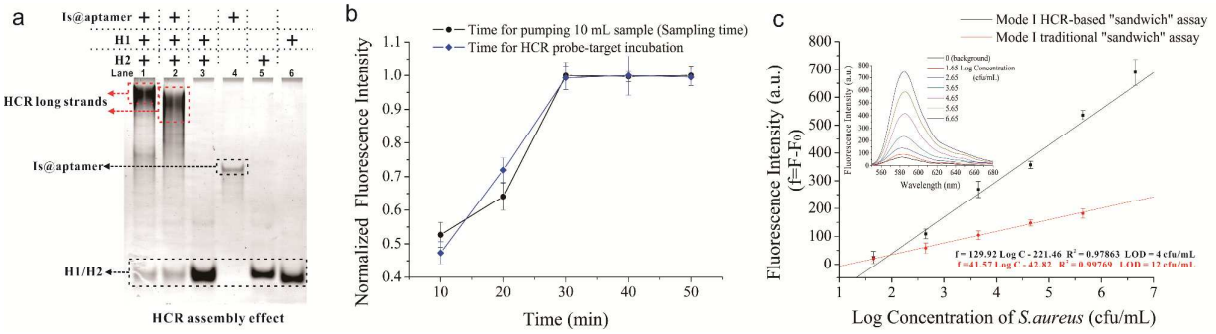

Figure 3. (a) PAGE analysis of HCR long amplified probe assembly in Mode I, where "+" represents the presence of corresponding sequences. For samples in Lane 1, 3, 4, 5, 6, corresponding DNA ingredients (100 nM Is@aptamer, 500 nM H1 and 500 nM H2) were mixed and annealed before assembly incubation. For the sample in lane 2, the three sequences were mixed and directly incubated at room temperature. **(b)** Sampling time and probe incubation time optimization with 4×10^5 cfu/mL *S. aureus* being detected in 3D chip Mode I analysis. The fluorescence intensity was normalized by dividing that of the maximum signal. **(c)** Standard curves of the HCR-based "sandwich" assay and traditional "sandwich" assay in Mode I with fluorescence intensity ($f = F\text{-}F_0$) versus the logarithmic concentration of *S.aureus*; F represents the fluorescent intensity of samples and F_0 represents the background when detecting buffer solution. The linear range of HCR-based and traditional "sandwich" assay are $4.5\times10\text{-}4.5\times10^6$ cfu/mL and $5\times10\text{-}5\times10^5$ cfu/mL respectively. Error bars in the calibration indicate the standard deviation (6 measurements). Inset: the fluorescence spectra of HCR-based "sandwich" assay.

- **3D chip for pathogenic bacteria detection based on HCR Mode II**

The rapid assembly HCR sequences. Apart from Mode I, another novel analytical strategy of signal amplification was also constructed. Importantly, in Mode II, the long amplified probe polymerizes on the inner surface of 3D chip, spending a period of time that should be counted in the analysis time scale. This makes it fatal to design a group of HCR sequences with rapid assembly speed. Plenty of works have been reported as HCR-based biosensors, in which the HCR assembly usually takes couple of hours.[19,32,33] Thus in the case of Mode II, we firstly proposed a group of HCR sequences with rapid assembly speed after trials of various designs. Figure 4a reveals the assembly effect of the ideal group and a relatively inferior group after a 20-minute room temperature incubation. Although there are some secondary structures of hairpin dimers in both ideal group and inferior group, the Is in ideal group quickly initiates the HCR polymerization (Lane 1) and the aptamer can greatly block the Is thus hindering the HCR assembly (Lane

2). Whereas, few polymerized double strands were assembled in the inferior group (Lane 6). We have carried out a series of comparative experiments (data not provided), and ultimately selected this ideal group for subsequent experiments. Some pioneering works have reported methods to speed up the self-assembly of DNA, such as using polar solvents[35] or high ionic strength buffer. Some guidelines were also established for HCR sequences design.[36] As shown in Figure 4a, the ideal group of sequences uses a stem length of 18 nucleotides (nt) to lock a 6 nt toehold. The CG content is 50-67% in the toehold domain, and is 50% in the stem. To further explore the mechanism of rapid HCR assembly, systematic computational exploration based on thermodynamic model is needed,[37] which is not covered in this work.

It is well-known that aptamer is susceptive to binding buffer. Aptameric biosensors may fail to function when the ionic strength or pH of binding buffer is changed. However, in Mode II, the aptamer-target interaction is carried out prior to HCR assembly. Therefore, the ionic strength of HCR buffer could be adjusted regardless of the harsh demand of aptamer, which accounts for an advantage of Mode II. The HCR assembly effect upon 15-min incubation in buffer solution with different Na^+ concentration (C_{Na^+}) was investigated. Figure 4b shows that the assembly speed raises with the increase of C_{Na^+}, and higher C_{Na^+} indicates more uniform long strands and less secondary structure of hairpin dimers. Therefore, a binding buffer with 800 mM Na^+ was used as the friendly condition for HCR probe assembly in Mode II.

It has been reported that hybridization efficiency of HCR might be negatively affected when Is was fixed on one end to a substrate.[24] Therefore, besides PAGE analysis, the HCR assembly speed was also investigated in an Au nanoparticles (AuNPs) system, where the 3' thiolated Is (SH-Is) was anchored on the surface of AuNPs. In this case, HCR occurred on the surface of AuNPs to form long assembled double strands. The H1/H2 were not modified with fluorophore. Instead, SYBR Green I was used to evaluate the amount of assembled double strands when measuring the fluorescent signal by fluorescence spectrophotometer. The detailed experiment description of this part is provided in Supporting Information. As shown in Figure 4c, the fluorescence signal got saturated when the Is functionalized AuNPs was incubated with H1 and H2 for 15 min.

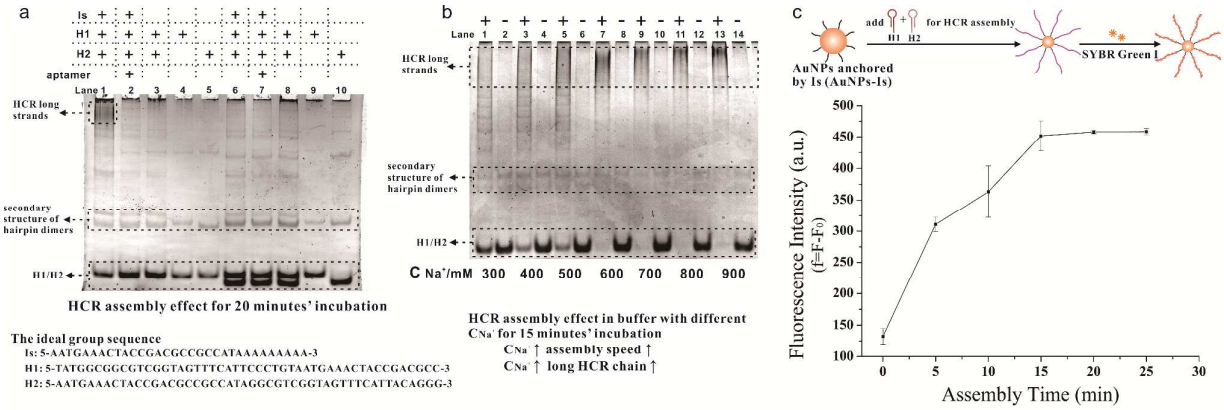

Figure 4. (a) Assembly effect of two groups of HCR sequences, Lane 1-5 for ideal group and Lane 6-10 for inferior group. All of the HCR groups were designed based on the sequence of aptamer, with 12 bases in Is complementary to the aptamer. 50 nM Is, 250 nM H1 and 250 nM H2 were used in these samples. For samples in Lane 1 and Lane 6, Is and H1/H2 were mixed and incubated for 20 min at room temperature. For samples in Lane 2 and Lane 7, 50 nM Is and 100 nM aptamer were incubated for 30 min before H1/ H2 being added. **(b)** Assembly effect in buffer with different Na^+ concentrations from 300 mM to 900 mM. "+" represents the assembly sample with 50 nM Is and 250 nM H1/H2 incubating for 15 min; "-" represents the control sample with 50 nM Is and 100 nM aptamer pre-incubating for 30 min before 15 minutes' HCR

assembly. **(c)** The AuNPs analysis of HCR assembly speed. The AuNPs-Is was incubated with H1/H2 for different time (0-25 min). For the 0-minute incubated sample, H1/H2 were added and immediately washed off by centrifugation. The fluorescence intensity represents the signal of each sample (F) subtracting the signal of the background (F_0).

Mode II principle confirmation. The rapid assembly HCR offers the prerequisite for Mode II. Then, the principle of Mode II was confirmed by PAGE analysis. As shown in Figure 5a, lane 1-6 indicate that the *S.* Typhimurium binds with aptamer but hardly binds with Is. Lane 7-10 show that the presence of aptamer blocks the Is and hinders the HCR assembly. However, adding *S.* Typhimurium can relieve the block and recover the HCR assembly. Similarly, the principle was also investigated in the AuNPs system. The experimental method of this part is described in Supporting Information. As illustrated in Figure 5b, the presence of aptamer greatly inhibits the HCR assembly, while adding the *S.* Typhimurium can relieve the block and recover the HCR assembly. It is noteworthy that the fluorescence recovery caused by bacteria-aptamer binding (column d) is not complete by comparing with the system without aptamer and *S.* Typhimurium (column b). This could be explained by the loss of AuNPs when centrifuging to separate bacteria-aptamer complex from the AuNPs. Part of the AuNPs with HCR long assembled double strands might precipitate with bacteria during centrifugation, leading to a bold depress in fluorescence signal.

Analytical performance of Mode II. The 3D chip for *S.* Typhimurium detection Mode II was carried out and its performance was evaluated. In particular, the amount of H1/H2 used in Mode II 3D chip assay was optimized. After the sample containing 1.7×10^6 *S.* Typhimurium was pumped and rinsed, H1 and H2 at different concentrations were added and incubated. Figure S-9 shows the fluorescence signal plateaus after 15-minute treatment with 4 μM H1 and 4 μM H2. Therefore, 5 μM H1/H2 were used throughout Mode II 3D chip assay. The sensitivity of Mode II in 3D chip was investigated. As shown in Figure 5c, Mode II in 3D chip assay exhibits a relatively higher limit of detection (LOD = 8 cfu/mL) compared with Mode I. A reasonable explanation of this phenomenon might be the different affinity of applied aptamers. Additionally, a bacterial cell can interact with multiple aptamers, as depicted in Figure 2, leading to multiple long amplified probes binding to one bacterial cell in Mode I, which caused a relatively higher signal comparing with Mode II. To define a positive result, we used $3\delta_b$ (60 a.u.) as reference. Commercially obtained non-fat milk powder and raw ground pork were spiked with *S.* Typhimurium for recovery analysis in this biosensor Mode II. The analysis result in Table S-3 shows no significant difference between the classical counting method and the proposed biosensor with the recovery ranging from 81.4% to 118.1%. The spiked *S.* Typhimurium was detected as positive result. Specificity of Mode II was also evaluated by detecting other serotypes of *S. enterica* and other bacteria as shown in Figure S-7b. Apparently, the proposed biosensor based on *S.* Typhimurium aptamer has limited ability to distinguish different serotypes of *S. enterica*. Other kinds of bacteria can also to some extent lead to net signal. Such limited specificity has been reported in the *S.* Typhimurium aptamer SELEX work,[38] as well as other aptamer application works.[39,40] It is expected that the multi-channel 3D chip can be used to combine multiple *S.* Typhimurium aptamers in different channels in order to improve the specificity.

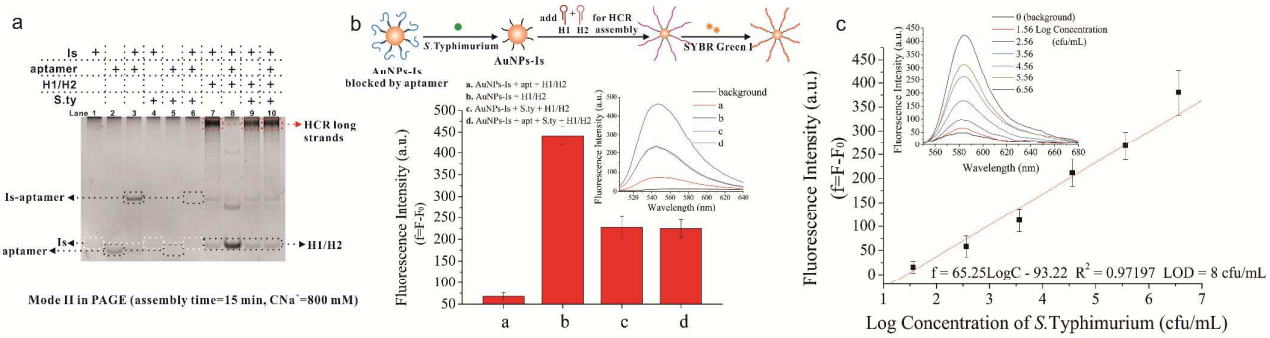

Figure 5. (a) The principle of Mode II in PAGE analysis. The cultures containing bacteria after an overnight fostering were centrifuged, washed, and re-suspended in equal volume of binding buffer to get *S.* Typhimurium sample. For Lane 1-6, 400 nM Is, 400 nM aptamer and *S.* Typhimurium sample were prepared in corresponding samples. *S.* Typhimurium in samples 4, 5, 6 was removed by centrifugation (5000 rpm, 2 min) before being loaded to the gel. For Lane 7-10, 75 nM Is, 150 nM aptamer, 300 nM H1/H2 and *S.* Typhimurium sample were prepared in corresponding samples. For sample in Lane 9, *S.* Typhimurium was firstly incubated with Is and removed by centrifugation before adding H1/H2. For sample in Lane 10, Is was firstly blocked by aptamer and then incubated with *S.* Typhimurium. After the *S.* Typhimurium binding with aptamer was removed, H1/H2 were added into the sample. **(b)** Mode II in AuNPs assay. The fluorescence intensity represents the signal of each sample (F) subtracting the signal of background (F_0). Inset shows the fluorescence spectra. **(c)** Standard curve of Mode II assay with fluorescence intensity ($f = F-F_0$) versus the logarithmic concentration of *S.* Typhimurium. F represents the fluorescent intensity of different samples and F_0 represents the background when detecting buffer. The linear range is $3.6\times10\text{-}3.6\times10^6$ cfu/mL. Error bars in the calibration indicates the standard deviation (6 measurements). Inset shows the fluorescence spectra.

Conclusion

In this study, a multi-channel structured 3D chip for pathogenic bacteria detection based on HCR signal amplification was developed. Acting as the analytical carrier, the 3D chip enables detection for large volume sample with low target concentration; offers large sensing area for target binding; possesses good optical condition for *in-situ* LIF system; and benefits the convenient analysis processes. Two modes of signal amplification based on HCR were constructed along with the 3D chip in this pathogenic bacteria biosensor. The long HCR amplified probe constructed under optimized condition was utilized in a "sandwich" assay format. This signal amplification Mode I guarantees an additional benefit for 3D chip sensitive detection. A novel format of HCR amplification in Mode II was also proposed, which provided more friendly condition for HCR assembly. Under such optimized condition, a group of rapid assembly HCR sequences was proposed. Both the two modes of analytical strategy were proved to be effective along with the 3D chip analytical carrier, and they are convenient and sensitive for whole cell pathogenic bacteria detection. Besides the two modes described in this work, we believe that the multi-channel structured 3D chip could be constructed with other analytical strategies to realize various pathogenic bacteria detection. It has potential to find applications in food safety monitoring as well as other analysis fields.

Associated Content

Supporting Information

The supporting information is available:

Reagents and materials; LIF system setup details; Bacteria strain and culture media; AuNPs assay protocol; Real sample assay protocol; Sequences used; SEM image of 3D chip; illustration of 3D chip and PMMA sheet comparison; DNA amount analysis of chip modification; optimization of long amplified probe assembly time, molar ratio and using amount in Mode I; specific analysis; characterization of AuNPs; optimization of H1/H2 amount in Mode II; recovery analysis

Acknowledgement

This research was gratefully supported by the National Natural Science Foundation of China (No. 21874095), National Recruitment Program of Global Experts (NRPGE), Graduate Student's Research and Innovation Fund of Sichuan University (No. 2018YJSY054), and Open Project of Animal Disease Prevention and Food Safety Key Laboratory of Sichuan Province.

References:

(1) National Office for Emergency Management: Official Webside of National Health and Family Planning Commission of PRC, **2016**.
http://www.nhfpc.gov.cn/yjb/s7859/201604/8d34e4c442c54d33909319954c43311c.shtml
(2) Mandal, P. K.; Biswas, A. K.; Choi, K.; Pal, U. K. *Am. J. Food Technol.* **2011**, *6*, 87-102.
(3) Váradi, L.; Luo, J. L.; Hibbs, D. E.; Perry, J. D.; Anderson, R. J.; Orenga, S.; Groundwater, P. W. *Chem. Soc. Rev.* **2017**, *46*, 4818-4832.
(4) Mauk, M.; Song, J.; Bau, H. H.; Gross, R.; Bushman, F. D.; Collman, R. G.; Liu, C. *Lab. Chip.* **2016**, *17*, 382-394.
(5) Ahmed, A.; Rushworth, J. V.; Hirst, N. A.; Millner, P. A. *Clin. Microbiol. Rev.* **2014**, *27*, 631-646.
(6) Yoo, S. M.; Sang, Y. L. *Trends Biotechnol.* **2015**, *34*, 7-25.
(7) Wu, S.; Duan, N.; Shi, Z.; Fang, C.; Wang, Z. *Anal. Chem.* **2014**, *86*, 3100-3107.
(8) Cho, I. H.; Mauer, L.; Irudayaraj, J. *Biosens. Bioelectron.* **2014**, *57*, 143-148.
(9) Vaisocherová-Lísalová, H.; Víšová, I.; Ermini, M. L.; T, Š.; Song, X. C.; Mrázek, J.; Lamačová, J.; Jr, S. L. N.; P, Š.; Homola, J. *Biosens. Bioelectron.* **2016**, *80*, 84-90.
(10) Meng, X.; Wang, H.; Chen, N.; Ding, P.; Shi, H.; Zhai, X.; Su, Y.; He, Y. *Anal. Chem.* **2018**, *90*, 5646-5653.
(11) Lee, W.; Kwon, D.; Choi, W.; Jung, G. Y.; Jeon, S. *Sci. Rep.* **2015**, *5*, 7717-7722.
(12) Duan, N.; Ding, X.; Wu, S.; Xia, Y.; Ma, X.; Wang, Z.; Chen, J. *J. Microbiol. Methods* **2013**, *94*, 170-174.
(13) Lee, W.; Kwon, D.; Chung, B.; Jung, G. Y.; Au, A.; Folch, A.; Jeon, S. *Anal. Chem.* **2014**, *86*, 6683-6688.
(14) Yu, Q.; Wang, X.; Duan, Y. *Anal. Chem.* **2014**, *86*, 1518-1524.
(15) Yan, X.; Wang, J.; Zhu, L.; Lowrey, J. J.; Zhang, Y.; Hou, W.; Dong, J.; Du, Y. *Lab. Chip.* **2015**, *15*, 2634-2646.
(16) Paniel, N.; Baudart, J.; Hayat, A.; Barthelmebs, L. *Methods* **2013**, *64*, 229-240.
(17) Wu, W.; Zhao, S.; Mao, Y.; Fang, Z.; Lu, X.; Zeng, L. *Anal. Chim. Acta* **2015**, *861*, 62-68.
(18) Zhang, P.; Liu, H.; Li, X.; Ma, S.; Men, S.; Wei, H.; Cui, J.; Wang, H. *Biosens. Bioelectron.* **2016**, *87*, 1044-1049.
(19) Dirks, R. M.; Pierce, N. A. *Proc. Natl. Acad. Sci. U. S. A.* **2004**, *101*, 15275-15278.
(20) Choi, H. M. T.; Beck, V. A.; Pierce, N. A. *Acs Nano* **2015**, *8*, 4284-4294.
(21) Huang, J.; Wang, H.; Yang, X. H.; Quan, K.; Yang, Y. J.; Le, Y.; Xie, N. L.; Ou, M.; Wang, K. M. *Chem. Sci.* **2016**, *7*, 3829-3835.
(22) Guo, Q.; Han, J. J.; Shan, S.; Liu, D. F.; Wu, S. S.; Xiong, Y. H.; Lai, W. H. *Biosens. Bioelectron.* **2016**, *86*, 990-995.
(23) Li, Z.; He, X.; Luo, X.; Wang, L.; Ma, N. *Anal. Chem.* **2016**, *88*, 9355-9358.
(24) Song, W.; Zhu, K.; Cao, Z.; Lau, C.; Lu, J. *Analyst* **2012**, *137*, 1396-1401.
(25) Ge, Z.; Lin, M.; Wang, P.; Pei, H.; Yan, J.; Shi, J.; Huang, Q.; He, D.; Fan, C.; Zuo, X. *Anal. Chem.* **2014**, *86*, 2124-2130.
(26) Bai, Y.; Koh, C. G.; Boreman, M.; Juang, Y. J.; Tang, I. C.; Lee, L. J.; Yang, S. T. *Langmuir* **2006**, *22*, 9458-9467.
(27) Kang, K.; Choi, J.; Nam, J. H.; Lee, S. C.; Kim, K. J.; Lee, S. W.; Chang, J. H. *J. Phys. Chem. B* **2009**, *113*, 536-543.
(28) Luo, Z.; Wang, Y.; Lu, X.; Chen, J.; Wei, F.; Huang, Z.; Zhou, C.; Duan, Y. *Anal. Chim. Acta* **2017**, *984*, 177-184.
(29) Yu, Q.; Zhan, X.; Liu, K.; Lv, H.; Duan, Y. *Anal. Chem.* **2013**, *85*, 4578-4585.
(30) Lee, S. H.; Ahn, J. Y.; Lee, K. A.; Um, H. J.; Sekhon, S. S.; Sun, P. T.; Min, J.; Kim, Y. H. *Biosens. Bioelectron.* **2015**, *68*, 272-280.
(31) Tang, Y.; Li, Z.; Luo, Q.; Liu, J.; Wu, J. *Biosens. Bioelectron.* **2016**, *79*, 715-720.
(32) Zhu, G.; Zhang, S.; Song, E.; Zheng, J.; Hu, R.; Fang, X.; Tan, W. *Angew. Chem.* **2013**, *125*, 5600-5606.

(33) Shuai, H. L.; Wu, X.; Huang, K. J.; Zhai, Z. B. *Biosens. Bioelectron.* **2017**, *94*, 616-625.
(34) Cao, X.; Li, S.; Chen, L.; Ding, H.; Xu, H.; Huang, Y.; Li, J.; Liu, N.; Cao, W.; Zhu, Y. *Nucleic Acids Res.* **2009**, *37*, 4621-4628.
(35) Kang, D.; Duan, R.; Tan, Y.; Hong, F.; Wang, B.; Chen, Z.; Xu, S.; Lou, X.; Wei, W.; Yurke, B.; Xia, F. *Nanoscale* **2014**, *6*, 14153-14157.
(36) Ang, Y. S.; Yung, L. L. *Chem. Commun.* **2016**, *52*, 4219-4222.
(37) Dirks, R. M.; Lin, M.; Winfree, E.; Pierce, N. A. *Nucleic Acids Res.* **2004**, *32*, 1392-1403.
(38) Joshi, R.; Janagama, H.; Dwivedi, H. P.; Senthil, T. K.; Jaykus, L. A.; Schefers, J.; Sreevatsan, S. *Mol. Cell. Probes* **2009**, *23*, 20-28.
(39) Sheikhzadeh, E.; Chamsaz, M.; Turner, A. P.; Jager, E. W.; Beni, V. *Biosens. Bioelectron.* **2016**, *80*, 194-200.
(40) Bagheryan, Z.; Raoof, J. B.; Golabi, M.; Turner, A. P.; Beni, V. *Biosens. Bioelectron.* **2016**, *80*, 566-573.

For Table of Contents Only